DYNAMIC BLOOD FLOW IN A LEFT VENTRICLE

Hidehito IWASE[1], Hao LIU[2], Shinichi FUJIMOTO[3], Ryutaro HIMENO[4]

[1]Computer Information Center and Advanced Engineering Center, RIKEN
2-1, Hirosawa, Wako-shi, Saitam 351-0198 Japan
e-mail, Iwase@postman.riken.go.jp
[2]Computer Information Center and Advanced Engineering Center, RIKEN
2-1, Hirosawa, Wako-shi, Saitam 351-0198 Japan
e-mail:hliu@postman.riken.go.jp
[3]Department of General Medicien and Nara Medical University
840 Shijo Kashihara Nara, 634-8522 Japan
[4]Computer Information Center and Advanced Engineering Center, RIKEN
2-1, Hirosawa, Wako-shi, Saitam 351-0198 Japan
e-mail:himeno@postman.riken.go.jp

Abstract

An efficient, image-based, computational modeling method for computational fluid dynamic study of left ventricle (LV) haemodynamics is presented. A Two-Chamber-View modeling method is proposed for reconstructing an anatomically realistic model of left ventricle, which is based on ultrasonographic images of two mutually perpendicular slice sections align with the long-axis. Each cross section of the short-axis is approximated as an ellipse with two radii determined from the extracted endocardial borderline, and is stacked up from the apex to the mitral- and aortic-valve planes to generate a fully three-dimensional geometric LV model. Physiological condition is also obtained based merely on the same ultrasonographic images; and the flow rates at mitral– and aortic valve are directly derived from the time-variation-rate of the LV volume. A computational fluid dynamic modeling of the left ventricle haemodynamics is further conducted; and the computed results indicate that realistic modeling of both geometry and physiological conditions of left ventricle is of great importance in correctly predicting the behavior of the strong vortex flow patterns and their influence on the heart function.

1. Introduction

The human heart plays a vital part in cardiovascular physiology, functioning as a pump to supply blood to the entire circulatory system. Many heart diseases are closely associated with the behavior of blood flow patterns in the heart chambers, in particular the left ventricle; and detailed haemodynamic information about the left ventricle can not only enhance our understanding of physiological function of the heart but also be very useful for certain clinical treatments. Although many physical, experimental and computational studies (1-6) have been conducted on the flow patterns in the left ventricle the, as a result of the highly unsteady movements and large deformation of the LV chamber wall and valves throughout diastole (filling) and systole (ejection), the LV haemodynamics , in fact, are not yet clearly understood.

Clinical visualization approaches such as Ultrasonography (US) and echo Doppler, Magnetic Resonance Imaging (MRI) may offer non-invasive, anatomically accurate, time-varying structure of the heart chambers but the modes are usually two-dimensional views of three-dimensional phenomena. However, combining the latest Computational Fluid Dynamics (CFD) techniques with *in vivo* data from the US and/or MRI could lead to advanced tools for visualization, examination, and diagnosis of the specific heart disorders and the effects caused by certain clinical treatments.

Our goal of this study is to establish methodology and framework for efficient, image-based, computational modeling of the left ventricle geometry based on ultrasonography approach and a CFD modeling of the LV haemodynamics. We address a Two-Chamber-View modeling method newly developed for reconstructing an anatomically realistic model of left ventricle, which is based on ultrasonographic images of two mutually perpendicular slice sections align with the long-axis. In this method, each cross section of the short-axis is approximated as an ellipse with two radii determined from the extracted endocardial borderline, and is stacked up from the apex to the mitral- and aortic-valve planes to form a fully three-dimensional geometric LV model. Physiological condition is also obtained merely based on the same ultrasonographic images; and the flow rates at mitral – and aortic valve are directly derived from the time-variation-rate of the LV volume. Computational fluid dynamic modeling of the left ventricle haemodynamics is conducted using a in-house, robust NS solver that is formulated in strong conservative form for both momentum and mass and is solved using a finite volume method. The computed results indicate that realistic modeling of both geometry and physiological conditions of left ventricle is of great importance in correctly predicting the behavior of the strong vortex flow patterns and their influence on the heart functions.

2. Morphological modeling

We have proposed a new method, the so-called Two-Chamber-View modeling method for reconstructing an anatomically realistic model of left ventricle chamber. This method is based on the ultrasonographic images of two mutually perpendicular slice sections align with the long-axis, that, as illustrated in Fig. 1, are named as 0 degree plane and 90 degree plane, respectively. Each cross section of the short-axis is approximated as an ellipse with two radii determined from the extracted endocardial borderline, and is stacked up from the apex to the mitral- and aortic-valve planes to form a fully three-dimensional geometric LV model. Information of the long-axis and the two radii of the ellipse are obtained and extracted from the LV outlines on the two planes.

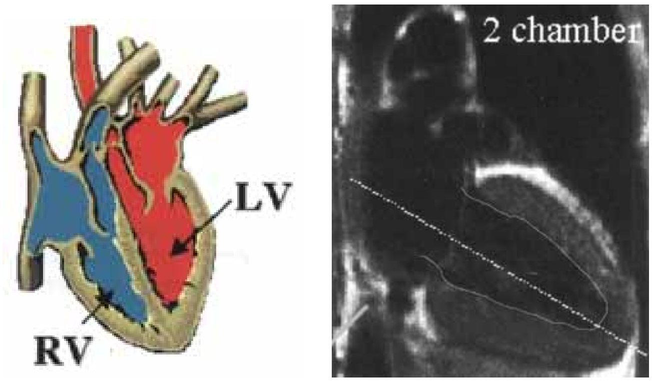

Fig. 1 Morphology of the heart and a two-chamber-view of the left ventricle

The procedure for reconstructing the left ventricular model is illustrated in Fig. 2 and described in details as below.

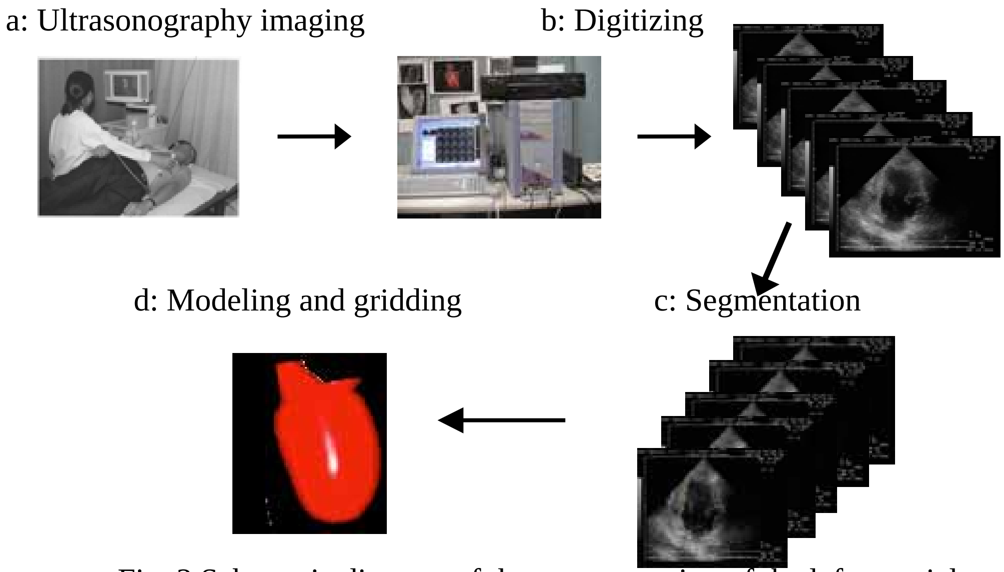

Fig. 2 Schematic diagram of the reconstruction of the left ventricle

Echocardiographic LV imaging and digitizing

The ultrasonographic imaging as shown in Fig. 2(a) is taken of a patient who is a 55 years old man with a healthy heart. The echocardiograms of the LV endocardial border on two mutually perpendicular planes named as 0 degree plane and 90 degree plane are taken and recorded into a VHS video tape with echocardiography. Then, the recorded left ventricle sequences are taken into a personal computer being digitized into a movie with 34 frames in a complete beat cycle, and further converted into a set of static images using commercial software of Adobe photoshop and Sony PictureGear.

Segmentation

Segmentation of the LV outline is done in two fold: 1) extracting the configuration of the LV endocardial borderline on two images at each frame (or time step); and subsequently 2) forming a spatial centerline curve along the long-axis with corresponding two radii at each cross section in the short-axis direction. The detailed procedure is as below.

We first extract the endocardial borderlines on two planes for all frames in a complete cycle manually and simultaneously store the dataset in a global coordinate system. Then, two ends of the mitral valve circle are connected with a straight line, which is defined as a reference line to determine the inclination angle of the mitral valve plane. And the extracted outlines are modified by a rigid rotation based on the calculated angle of the mitral valve plane so that the reference line becomes horizontal. The length between the apical point and the center point of the mitral valve is defined as the LV height. Here, a temporary LV centerline is defined running along the straight line between the two points. Furthermore, we scan the LV endocardial borderline vertically from the apex up to the mitral valve with a uniform spacing to search the borderline points. In case of that more then two pixel points come out a thinning treatment is conducted so that only two points are finally selected. Eventually, averaging the extracted two borderline points give the coordinates of the LV centerline as well as two radii of the ellipse at the corresponding cross section. In this study, forty elliptical cross sections are generated and stacked up with uniform interval to generate a complete three-dimensional geometric model of the LV. Repeating this procedure for all the frames we can eventually get a realistic LV model that deforms with time. Additionally, the inner diameters of the mitral valve and the aorta valve are also measured by echocardiography and attached onto the reconstructed LV model.

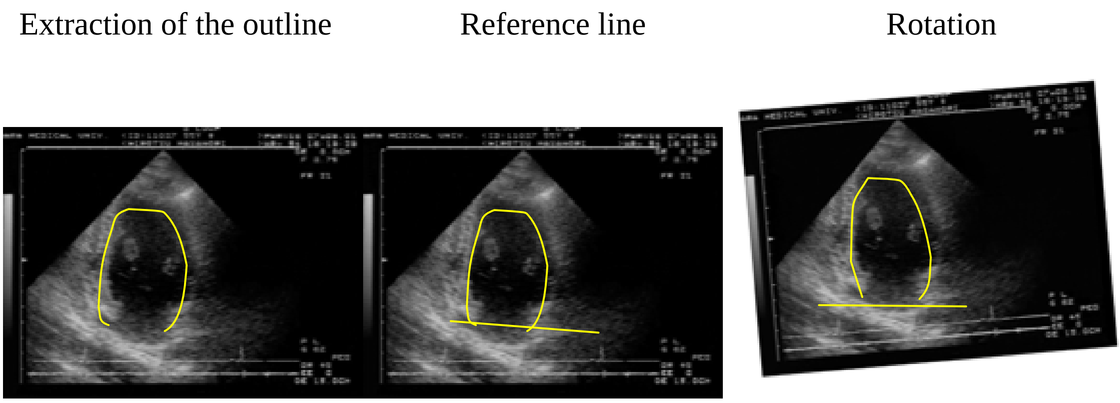

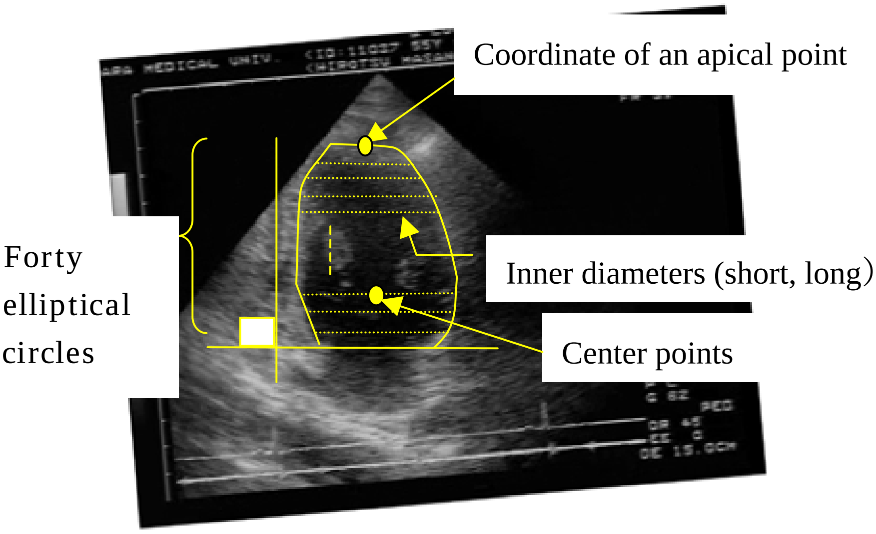

Fig. 3. Schematic diagram of the segmentation of the LV

Smoothing

Since the raw US images usually involve some noises and may be not clear the outlines being extracted accordingly need to be smoothened in an appropriate way. This smoothing is, in general, carried out in both space and in time. There are many ways to make the spatial smoothing of the outlines. We employed a simple but effective method to merely smoothening the points along the long-axis such as,

$$D_i^t = \frac{d_{i-1}^t + d_i^t + d_{i+1}^t}{3.0}, \qquad (1)$$

where d may express the old coordinate (x, y, z) or diameter, D is the new coordinate or diameter, and the subscribe i is denotes the numbered point.

With the smoothing in time we utilized the same method for the extracted two outlines at each time step or frame, i.e.,

$$da_i^t = \frac{D_i^{t-1} + D_i^t + D_i^{t+1}}{3.0} \qquad (2)$$

where a is the coordinate or diameter finally used in modeling of the LV.

Note that synchronization of images as well as the extracted outlines on the 0- and 90-degree plane is necessary because these images are time-dependent and measured at different moment. This is done by comparing the time-variation of the areas of the extracted outlines of the LV rated in Fig. 3.

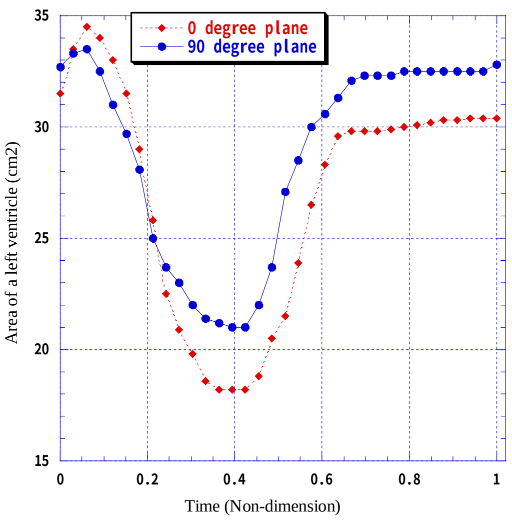

Fig.4 Synchronization of dataset between 0 degree and 90 degree images

Modeling and gridding

Using the synchronized outline data of the LV we then calculate the coordinates of the centerline (xc, yc, zc) as well as the two radii of each elliptical cross section. One heartbeat cycle is divided into thirty-four time steps in a uniform way. At each time step a wire-frame model is then constructed by stacking up the forty ellipses along the LV centerline and a H-type structured grid system is generated using a commercial grid generator, the Gridgen, VINAS Co., Ltd. Totally, thirty four grid systems are generated separately in a beat cycle as shown in Fig. 5. The grid system at any moment during a cycle can be interpolated in a linear way by using the grid systems at two adjacent time steps out of the thirty steps or in a nonlinear way based on a decomposed Fourier series with respect to time.

Note that the following issues are considered in the modeling of the LV. The diameters at mitral valve (Dmv) and aortic valve (Dav) are fixed during the LV contraction as well as the linkage portion between them. The ratio between the two diameters is about 0.8. A virtual entry region at the mitral valve is added up, which is 0.5 Dmv long with a constant diameter and the centerline points to the apex. A virtual outlet region is also made at the aortic valve, which is 1.5 Dav long and decreases down to the aortic diameter in a linear way. The coordinate origin is fixed at the center point of the outlet. Note that no valve is modeled here but influence of the mitral valve plane and the aortic valve plane are actually accounted for in the computational fluid dynamic modeling as described in the following section.

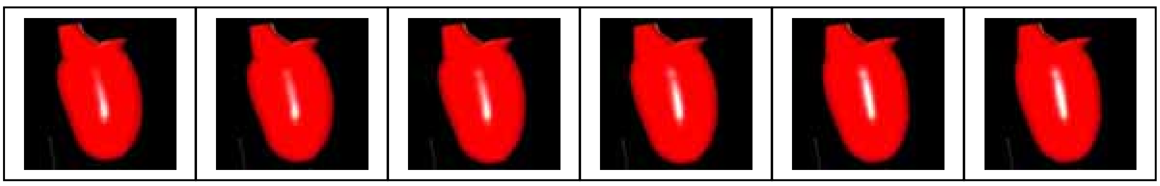

(1) (2) (3) (4) (5) (6)

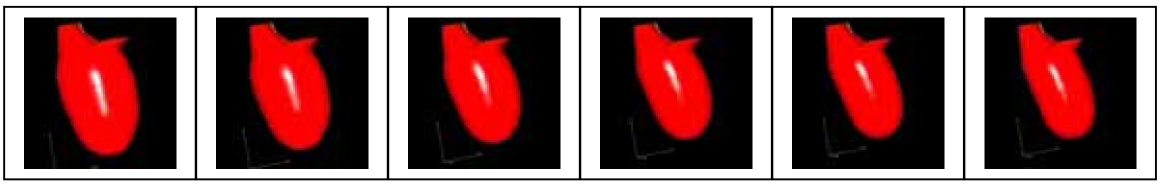

(7) (8) (9) (10) (11) (12)

Fig. 5 Morphological model and grid systems of the LV

3. Physiological modeling

Appropriate definition of physiological conditions for computational fluid dynamic modeling of LV haemodynamics is important, that may involve velocity and pressure conditions at mitral and aortic valves. Since the *in-vivo* pressure measurement is usually not feasible the velocity-based boundary condition is employed. In the following we described two methods to define the velocity boundary conditions.

US Doppler-based measurement of velocity

Definition of velocity conditions at inlet of mitral valve is straightforward, that may be simply realized by imposing the measured velocity profile at diastole when the mitral valve opens. The mean velocity profile is measured using US echo Doppler and converted into a set of points in which time-variation of the velocity in a beat cycle was plotted as shown in Fig. 6. The velocity at any moment during a cycle can then be interpolated in a linear way by using the velocities at two adjacent time steps or in a nonlinear way based on a decomposed Fourier series with respect to time. At aortic valve, no velocity is measured and imposed because the aortic valve is treated as outlet of the LV chamber.

As the opening and closing of the two valves are archived suddenly and prescribed as well as the movements of the LV wall the timing of the open and closure is defined as and controlled by three specific times, i.e., the Tmo (the moment when the mitral valve is opening), Tao (the moment when the aortic valve is opening), and Tac (the moment when the aortic valve is closing).

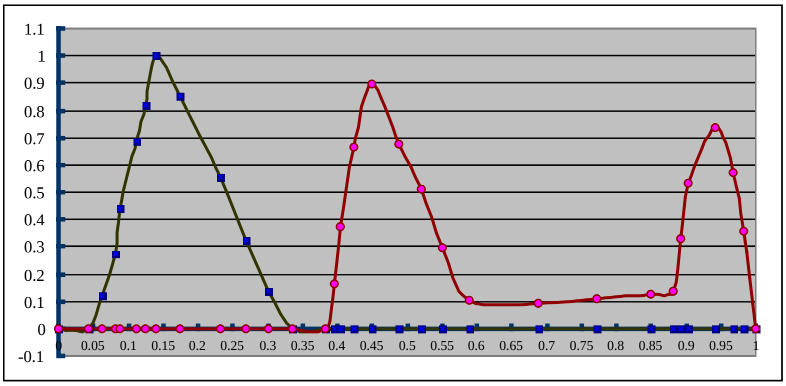

Fig. 6 US echo Doppler-based velocity at mitral –and aortic-valve

Image-based velocity

With consideration of the conservation of mass and momentum associated with the blood fluid inside the LV, the inflow and outflow velocities at mitral and aortic valves may also be derived directly from the time-variation of the LV volume completely based on the images. Firstly, the time-variation of the LV volume against time Vlv(t) can be calculated based on the thirty-four grid systems in a complete beat cycle as a summation of all the cell volumes at each time step. Then, the time-variation-rate of the volume dVlv(t)/dt is calculated as the volumetric flow rate at the mitral valve when it is positive at diastole or at the aortic valve when it is negative at systole. The velocity is hence obtained by directly dividing the time-variation-rate of the LV volume by the area of mitral valve plane or the aortic valve plane. Fig. 7 shows the time variation of the LV volume and the volumetric flow rate against time. The volumetric flow rate corresponds to the velocity at either mitral valve or aortic valve and shows very good agreement with the *in vivo* measurements. Feasibility of the image-based prediction of the velocity boundary condition has big merit and potential because we can construct geometric model and define flow conditions simultaneously, that would largely reduce both time and efforts from the clinical viewpoint and also can enhance the matching between computational modeling and physiological conditions.

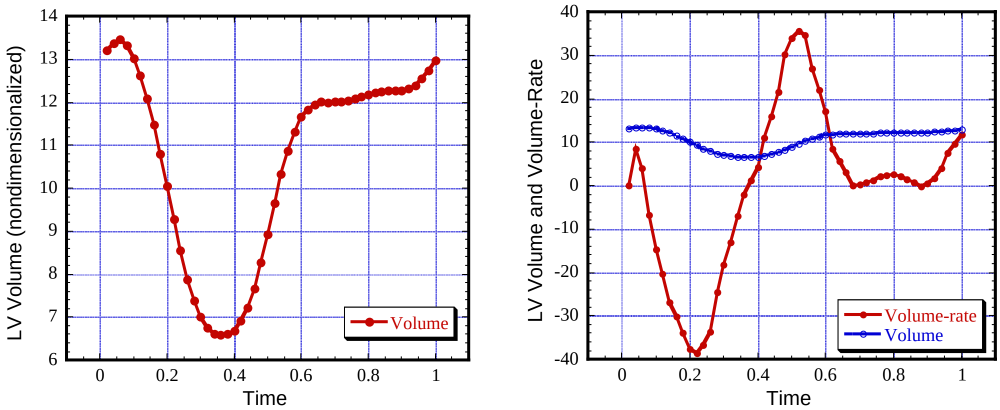

Fig. 7 Time variation of the LV volume and volumetric flow rate versus time

4. Haemodynamic simulation

A computational fluid dynamic modeling of the left ventricle is then carried out. Velocity at aortic valve is used as reference velocity; and aortic valve diameter is reference length. The Reynolds number is defined as $Re=Q_p/\upsilon$ where Q_p is the peak or mean volumetric flow rate at aortic valve and υ is the kinematic viscosity of the fluid. The Strouhal number is given by $St=d^2/Q_pT$ where d is the diameter of the aortic valve plane and T is the period of a complete cycle. The coordinates are scaled on d and the time on T. The Reynolds number is about 6000 when using the peak volumetric flow rate but 1000 in terms of time-averaged volumetric flow rate. The Strouhal number is 0.1 or 0.6, correspondingly.

Solutions to the Navier-Stokes equations

The fluid is assumed to be homogeneous, incompressible and Newtonian. The governing equations are the 3D incompressible, unsteady Navier-Stokes equations in the strong conservative form for momentum and mass, non-dimensionalized and written in a generalized curvilinear coordinate system, such that:

$$\int_{V(t)} St\left(\frac{\partial \boldsymbol{q}}{\partial \tau}\right) dV + St\frac{\partial}{\partial t}\int_{V(t)} \boldsymbol{Q} dV + \oint_{S(t)} \left(\boldsymbol{f} - \boldsymbol{Q}\boldsymbol{u_g}\right)\cdot \boldsymbol{n}\, dS = 0\,, \tag{3}$$

where the last term $f=(F+F_v,\ G+G_v,\ H+H_v)$ expresses the net flux across the cell faces. Other terms are defined as:

$$\boldsymbol{Q} = \begin{bmatrix} u \\ v \\ w \\ 0 \end{bmatrix} \boldsymbol{q} = \begin{bmatrix} u \\ v \\ w \\ p \end{bmatrix} \boldsymbol{F} = \begin{bmatrix} u^2 + p \\ uv \\ uw \\ \beta u \end{bmatrix} \boldsymbol{G} = \begin{bmatrix} vu \\ v^2 + p \\ vw \\ \beta v \end{bmatrix} \boldsymbol{H} = \begin{bmatrix} wu \\ wv \\ w^2 + p \\ \beta w \end{bmatrix},$$

$$\boldsymbol{F_v} = -\frac{1}{Re}\begin{bmatrix} 2u_x \\ u_y + v_x \\ u_z + w_x \\ 0 \end{bmatrix} \boldsymbol{G_v} = -\frac{1}{Re}\begin{bmatrix} v_x + u_y \\ 2v_y \\ v_z + w_y \\ 0 \end{bmatrix} \boldsymbol{H_v} = -\frac{1}{Re}\begin{bmatrix} w_x + u_z \\ w_y + v_z \\ 2w_z \\ 0 \end{bmatrix}. \tag{4}$$

In the preceding equations, p is pressure; u and v are velocity components in Cartesian coordinate system, x, y, and z; t denotes physical time; τ is pseudo time; $S(t)$ denotes the surface of the control volume; $\boldsymbol{n}=(n_x, n_y, n_z)$ are components of the unit outward normal vector corresponding to all the faces of the polyhedron cell, and Re is the Reynolds number. Note that, in the third component of Eq. (3), the method of pseudo-compressibility, is employed with a time derivative of pressure artificially added to the equation of continuity with a positive parameter β . Note that the term $\boldsymbol{q}$ associated with the pseudo time is designed for an inner-iteration at each physical time step, and will vanish when the divergence of velocity is driven to zero so as to satisfy the equation of continuity. The ALE method is introduced to deal with problems with boundaries moving and/or deforming with time, that results in a contribution from moving grid velocity as $\boldsymbol{u_g}$ in the last term in Eq. (3). The governing equations are discretized using the finite volume method (FVM) and are solved in a time-marching manner. A third-order upwind differencing scheme, using the flux-splitting method, is implemented for the convective terms in a MUSCL fashion. The viscous terms are evaluated using a second-order central differencing method based on a Gauss integration in the FVM manner. An implicit approximate-factorization method, based on the Euler implicit scheme, is employed for the discretization of the time derivatives. Details of the methods can be found in Liu [7].

On the solid wall of the left ventricle and the valve planes when they are closed we apply the non-slip condition for velocity components in which fluid has the same velocity as the moving wall does, and zero-gradient condition for pressure:

$(u, v) = U_{wall}$, and $p_n=0$, (5)

where subscript *n* denotes the unit normal vector at the wall stencils. At inlet, i.e., the mitral valve when it opens a uniform inflow is taken as:

$(u, v) = U_{mv}(t)$, and $p_n=0$. (6)

At outlet, i.e., the aortic valve when it opens the velocity gradient and the pressure are fixed to zero as:

$(u, v)_n = 0$, and $p=0$. (7)

The initial condition is that the flow in side the LV is at rest at t=0.

Results and discussions

Fig. 8(a)-(g) shows the vortical flow patterns in the LV model in a heart beat cycle. At early diastole, when the mitral valves open a strong jet is observed as shown in Fig.8(a), rushing into the left ventricle down to the apex. Then, two intense vortices(Fig.8(b)-(d)) are detected along with the jet stream that have different size and forms an asymmetric vortex ring in 3D structure. showing very good qualitative agreement compared with the MR images by Kilner et al(5). Overall a large vortex is detected in the centre of left ventricle(Fig.8(b)), and a small vortex is observed in the right part of left ventricle as shown in Fig. 8(c). The two vortices deform simultaneously while the second jet goes into the LV at late diastole(Fig.8(d)).

After the closure of the mitral valves the vortex flow inside the LV are still observed and during of iso-volume systole a rapid lift-up in pressure is detected, eventually forming a steep pressure gradient immediately before the systole. Subsequently, the aortic valves are forced to open and a very strong jet is pushed out as illustrated in Fig.8(e). The left vortex observed at diastole mainly forms the primary flow of the jet but the second vortex very likely contributes more to the secondary flow (Fig.8(f)). At late systole, the pressure in the left ventricle turns out to drop down to the aortic pressure and eventually leads to the closure of the aortic valve. Overall, our results indicate that the intense vortex flow pattern in the LV strongly depend upon the wall movement,i.e., the LV dynamics as well as the 3D geometry of realistic LV model.

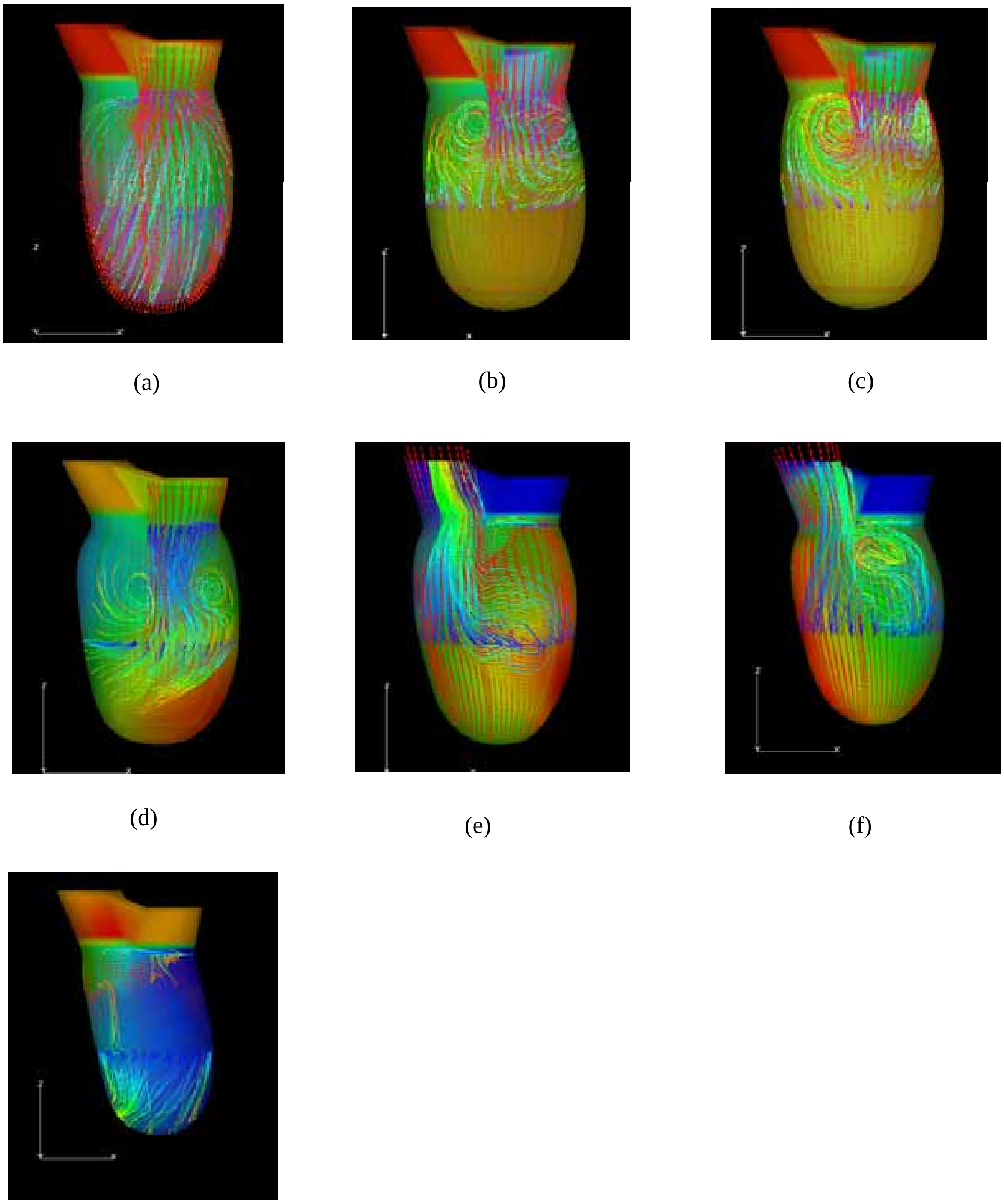

(a) (b) (c)

(d) (e) (f)

(g)

Fig. 8 Vortex flow patterns in a LV model

4. Conclusions

The present work demonstrates the feasibility and efficiency of an image-based, computational method for modeling of left ventricle in terms of time-varying realistic geometric model and physiological conditions. Implementation of the ultrasonographic image-based LV reconstruction is successfully archived by a Two-Chamber-View modeling method. Computed results of the left ventricle haemodynamics indicate that the strong vortex flow patterns strongly depend upon the LV wall movements in terms of both three-dimensional characteristics and timing.

References

(1) Peskin, C. S. and McQueen, D. M., A general method for the computer simulation of biological systems interacting with fluids, Symp. Soc. Exp. Bio., 49, 265-276, 1995.

(2) Taylor, T. W. and T. Yamaguchi., Realistic three-dimensional left ventricular ejection determined from computational fluid dynamics, Med. Eng. Phys., 17, 602-608, 1995.

(3) Fujimoto, S., Mizuno, R., Hashimoto, T., Dohi, K., Hirai, A. Nakanishi, S., and Nakano, H., Contribution of velocity profiles at the left ventricular outflow tract to calculations of stroke volume: A magnetic resonance imaging study, Echocardiography: A J. of CV Ultrasound & Allied Tech, 16 (1), 11-16, 1999.

(4) Lemmon, J. D. and Yoganathan, A. P., Computational modeling of left heart diastolic function: Examination of ventricular dysfunction, J. Biomech. Eng., 122, 297-303, 2000.

(5) Kilner, P. J., Yang, G. Z., Wikes, A. J., Mohiaddin, R. H., Firmin, D. N., and Yacoun, M. H., Asymmetric redirection of flow through the heart, Nature, 404, 759-761, 2000.

(6) Saber, N. R., et al., Computational flow modeling of the left ventricle based on in vivo MRI data: initial experience, Ann. Biom. Eng., 29, 275-283, 2001.

(7) Liu, H. and Yamaguchi, T., Waveform dependence of pulsatile flow in a stenosed channel, *J. Biomech. Eng.*, 123, 88-96, 2001.